THERMAL ENVIRONMENT OF RESIDENTIAL COMMUNITIES OVER A COAST AREA IN SOUTHEASTERN CHINA

F. Chen [1, 2], X.W. Shen[1], D.F. Huang[3], Y.X. Huang[4]

[1]College of Computer and Information Engineering, Xiamen University of Technology, 361024Xiamen, China -
(chenfeng@xmut.edu.cn; chenfeng105@gmail.com)
[2]Big Data Institute of Digital Natural Disaster Monitoring in Fujian, Xiamen University of Technology, 361024Xiamen, China
[3]Xiamen Hi-tech Innovation Centre, 361013Xiamen, China - dfhuang@xmibi.com
[4]Xiamen Meteorological Disaster Prevention Technology Center, 361013Xiamen, China - 1815963455@qq.com

ISPRS TC III and IV

ABSTRACT:

The characters of the residential communities over Tong'an District of Xiamen City in thermal environment as well as in biophysical factors were investigated mainly based on the Lansat-8 OLI/TIRS Collection 2 Level-2 products. Specifically, the surface temperature product was used in measuring thermal environment, and the surface reflectance product was used to derive biophysical factors through the tasseled cap transformation as well as the normalized difference vegetation index (NDVI). Among the four types of residential community, the old community in urban area was generally lower in NDVI and in the Wetness component and therefore had higher surface temperature. Varied relationships of surface temperature with biophysical factors among four types were observed, which also demonstrated seasonal variation. At the same time, the preliminary investigation showed that the residential communities located in rural-urban fringe and a small portion of village communities had confronted with problems in thermal environment as well as in surface biophysical conditions. Furthermore, limitations of this study were discussed, mainly in spatial resolution and temporal representativeness of the Landsat-8 OLI/TIRS data, in biophysical components derived from the multi-spectral reflectance without depicting actual landscape, and in no consideration for the background of individual community. As the whole district covers wide and complex territory along with different local climate types, more investigations in details are required.

1. INTRODUCTION

Thermal environment is widely regarded as an important factor in influencing people's physical and mental health (Patz et al., 2005), and as a valuable indicator associated with weather and climate change. In particular, of issues on the thermal environment over urban area, urban heat island (UHI) effect is observable globally, a phenomenon that urban area is usually provided with higher temperatures compared against its rural surroundings (Voogt and Oke, 2003). Currently, many studies have been conducted in monitoring and understanding UHI, with intention to find suitable or effective measures to mitigate its adverse influence and to enhance the capacity in urban sustainable development (Du et al., 2021). Generally, there are different types of urban heat island, mainly including surface UHI (SUHI), canopy UHI (CUHI), boundary UHI, and sub-surface UHI, while the SUHI and CUHI have been most investigated and compared (Voogt and Oke, 2003; Du et al., 2021). Particularly, the SUHI is based on land surface temperature (LST) usually obtained from the remotely sensed thermal infrared data. The remotely sensed LST is easily accessible over a large area, showing advantage compared against the *in-situ* measurement. Accordingly, the remotely sensed LST has been popularly implemented for urban thermal environment issues in scientific investigations and for administration purposes (e.g., urban planning and monitoring) (Weng, 2009). Currently, a large number of researches have been carried out to reveal the urban LST (or SUHI) pattern and changes, based on the remotely sensed observations. However, most of these studies have taken urban area as a whole, with exploring mainly the relationship of urban thermal environment

with several typical factors (e.g., land use and land cover, impervious surface, and vegetation). As a result, general findings were usually obtained. Meanwhile, some researches were mainly discussed at pixel scale. The pixel-based findings are generally hard to be interpreted for urban planning and management (Wilson et al., 2013). In other words, these findings are probably inadequate and not readily available for application. Residential community, as a living and social unit, is one of several tools planners use to control physical characteristics of developing landscapes by imposing restrictions, which consequently affect some environmental processes. That is to say, compared with the pixel scale of originally remotely sensed imagery, residential community unit (scale) is more appropriate for exploring the thermal environment from the perspective of practical application. Actually, residential communities show differences in several aspects among each other (e.g., construction age, construction materials, and landscape layout), and are provided with different backgrounds both in natural and cultural. Furthermore, with continuous urbanization and socioeconomic development, residential conditions in rural-urban fringe and rural areas far away from urban centers have also gone through environmental changes.

In this study, taking Tong'an District of Xiamen City over the southeast coast of China as a case, four types of residential community were grouped and selected, specifically including the newly built community in urban area (NCU), the old community in urban area (OCU), the mixed community in the rural-urban fringe (MC), and village community in rural area (Figure 1). The thermal environment of these residential communities and related surface characteristics were

investigated mainly by virtue of multi-temporal Landsat-8 OLI/TIRS observations. The satellite derived LST served as indicator in measuring thermal environment. Meanwhile, the components through the tasseled cap transformation (TCT) as well as the normalized difference vegetation index (NDVI), were implemented to describe the biophysical features of residential community.

2. DATA AND METHODS

2.1 Study Area and Typical Residential Communities

Tong'an District locates in the north of Xiamen City, along the southeast coast of Fujian Province, China. With a total land area about 669 km^2 (nearly accounting for 40% of the whole city), it can be roughly divided into three regions: the middle and low mountainous area in the north and northwest, the middle and low hilly area in the center, and the plain. It has a subtropical marine monsoon climate, with abundant rainfall and heat. In particular, with the change of altitude and landform, it can be divided into three climate types, including coastal, plain, northern and northwestern mountainous areas. In 2021, the resident population of Tong'an District was about 0.89 million. Currently, Tong'an District has jurisdiction over seven streets and four towns, specifically including 61 communities and 81 village committees which serve as basic administrative units in urban and rural areas respectively (http://www.xmta.gov.cn). Resulted from complex topography and continuous development with long history, different patterns of architectural landscape within and around residential areas are observable in Tong'an District, presenting both inter-class and intra-class differences (Figure 1).

Figure 1. Typical residential communities in Tong'an District. (a)~(c): Newly built community in urban area (NCU); (d)~(f): Old community in urban area (OCU); (g)~(i): Mixed community in the rural-urban fringe (MC); (j)~(l): Village community in rural area (VC).

In this study, typical residential communities of each type were collected. Specifically, the samples of NCU and OCU were inquired and collected through a online housing transaction platform (https://xm.58.com), of which the name, location and other attribute information were obtained. The samples of MC and VC were determined according to the administrative division information and the urban-rural division code. Finally, there were 20 NCUs, 21 OCUs, 20 MCs, and 20 VCs collected for further investigation. It is interested to compare these residential communities quantitatively in terms of biophysical properties and thermal characteristics, and to understand the relationship between these two aspects. To this end, related variables retrieved from remotely sensed imagery were used (see Section 2.2).

2.2 Data

Specifically, the thermal environment of these residential communities and related surface characteristics were investigated mainly by virtue of multi-temporal Landsat-8 OLI/TIRS observations. The satellite derived LST served as indicator in measuring thermal environment (see Section 2.3). Meanwhile, the TCT based biophysical components as well as the NDVI (see Section 2.4), were implemented to describe the biophysical features of residential community. In particular, multi-spectral information (i.e. of the Landsat-8 OLI) is usually decomposed into three components through the TCT, which called "Brightness", "Greenness", and "Wetness" respectively (see Section 2.5).

In this investigation, three scenes of the Landsat-8 OLI/TIRS Collection 2 Level-2 products were used (Table 1), including surface reflectance and surface temperature science products. In Collection 2 Level-2 products currently, for the Landsat-8 OLI/TIRS, the surface temperature was estimated using the Landsat surface temperature algorithm (Version 1.3.0), whereas the surface reflectance products were generated using the Land Surface Reflectance Code (LaSRC) algorithm (Version 1.5.0) (https://www.usgs.gov/landsat-missions/landsat-collection-2-level-2-science-products). In particular, the surface temperature products were retrieved with auxiliary information from other external data sources, mainly including atmospheric profiles of geopotential height, specific humidity, and air temperature as well as surface emissivity product (Cook et al., 2014).

Product type	Acquisition time
Collection 2 Level-2 (Landsat-8 OLI/TIRS) surface reflectance and temperature	August 4, 2013
	July 25, 2021
	December 16, 2021

Table 1. Data used in this study. The Landsat Collection 2 Level-2 Surface Reflectance and Surface Temperature scene-based products were freely assessed from EarthExplorer (https://earthexplorer.usgs.gov/).

2.3 Land Surface Temperature

As mentioned before, land surface temperature obtained through remotely sensed observations, especially the Landsat observations (e.g., Landsat-7 ETM+, Landsat-8 OLI/TIRS), has been popularly implemented for urban thermal environment issues. Specifically, several methods have been developed to retrieve LST from the Landsat-8 OLI/TIRS data (Jiménez-Muñoz et al., 2014; García-Santos et al., 2018), for which other auxiliary inputs are required. However, for ordinary data users,

it is impossible to get these inputs accurately and adequately in most cases, especially when LST over urban area is considered (Chen et al., 2016, 2017). At the same time, to alleviate this burden on ordinary data users, the Landsat Collection 2 Level-2 science products have been generated, mainly including surface reflectance product and surface temperature product (USGS, 2022). Accordingly, in this study the Landsat-8 Collection-2 Level-2 science products were collected and used instead of processing raw data step-by-step.

Specifically, to obtain LST from the Collection-2 Level-2 surface temperature product, following equation was used (USGS, 2022):

$$LST = 0.00341802 \times DN_{LST} + 149.0 - 273.15 \qquad (1)$$

where LST is the surface temperature (in °C), and DN_{LST} is the value recorded in the Collection 2 Level-2 surface temperature product. By the way, the surface temperature product is derived mainly from the TIRS Band 10 data with other auxiliary inputs, through a single channel algorithm (USGS, 2022).

2.4 Normalized Difference Vegetation Index

Spectral index retrieved from remotely sensed imagery is usually used as a practical way to delineate surface cover or status. In particular, the NDVI measures the contrast between the near-infrared (NIR) channel and Red channel in reflectance (Eq. (2)). The NDVI is considered as one of the most commonly used vegetation indices, which provides a standardized method in mapping vegetation greenness from satellite data (Chen et al., 2019).

$$NDVI = \frac{(Ref_{NIR} - Ref_{Red})}{(Ref_{NIR} + Ref_{Red})} \qquad (2)$$

where $NDVI$ is the normalized difference vegetation index estimated from the surface reflectance over near-infrared region (Ref_{NIR}) and red region (Ref_{Red}). Specifically, for the Landsat-8 OLI used here, Ref_{NIR} and Ref_{Red} are reflectance of Band 4 and Band 5 respectively.

In addition, to get the surface reflectance from the Collection 2 Level-2 surface reflectance product, following equation was used (USGS, 2022):

$$Ref = 0.0000275 \times DN_{Ref} - 0.2 \qquad (3)$$

where Ref is the surface reflectance, and DN_{Ref} is the value recorded in the Collection 2 Level-2 surface reflectance product.

2.5 Tasseled Cap Transformation

The tasseled cap transformation has been widely used to generate spectral features readily interpretable from multi-spectral observation, which directly relate to the physical parameters of land surface (Chen et al., 2020). Similar to NDVI, the spectral features through TCT provide a form of data reduction with no physical units (Zhai et al., 2022). Meanwhile, compared against the spectral index (i.e. NDVI), the TCT has an advantage in reducing data volume with minimal information loss (Crist and Cicone, 1984). The TCT components have been widely used in characterizing land surface properties and their dynamics (Chen et al., 2020; Zhai et al., 2022). Currently, there have been different versions of TCT developed for Landsat

observations (Chen et al., 2020), and a version for the Landsat-8 OLI surface reflectance has been newly published (Zhai et al., 2022). Through the TCT, the multi-spectral information recorded by the Landsat-8 OLI imagery is decomposed into three major components, which specifically are Brightness (Eq. (4)), Greenness (Eq. (5)), and Wetness (Eq. (6)) (Zhai et al., 2022). In particular, the Greenness is considered a good indicator for vegetation (e.g., coverage, status), while the Wetness is assumed to capture soil moisture or water content.

In this study, the TCT (Eq. (4)－Eq. (6)) was performed on the Landsat-8 OLI multi-spectral channel reflectance obtained from the Collection 2 Level-2 surface reflectance product (Eq. (3)).

$$Brightness = 0.3690 Ref_{Blue} + 0.4271 Ref_{Green} + 0.4689 Ref_{Red} \qquad (4)$$
$$+ 0.5073 Ref_{NIR} + 0.3824 Ref_{SWIR1} + 0.2406 Ref_{SWIR2}$$

$$Greenness = -0.2870 Ref_{Blue} - 0.2685 Ref_{Green} - 0.4087 Ref_{Red} \qquad (5)$$
$$+ 0.8145 Ref_{NIR} + 0.0637 Ref_{SWIR1} - 0.1052 Ref_{SWIR2}$$

$$Wetness = 0.0382 Ref_{Blue} + 0.2137 Ref_{Green} + 0.3536 Ref_{Red} \qquad (6)$$
$$+ 0.2270 Ref_{NIR} - 0.6108 Ref_{SWIR1} - 0.6351 Ref_{SWIR2}$$

where all spectral channels of the Landsat-8 OLI except two channels over Coastal/Aerosol and Cirrus were used in performing the TCT. Specifically, Ref_{Blue}, Ref_{Green}, Ref_{SWIR1}, and Ref_{SWIR2} are surface reflectance in Blue, Green, and shortwave infrared spectral regions, which are Band 2, Band 3, Band 6, and Band 7 of the Landsat-8 OLI respectively.

3. RESULTS AND DISCUSSION

For a residential community, the mean value of variable (LST or biophysical parameter) for the pixels correspondingly in space was taken to serve as representative. The preliminary findings show general differences among four types of residential community in thermal environment and in the biophysical components (Figure 2). By the way, most NCU communities selected had not been built and used until the end of 2020, which were not considered therefore in analyzing the data acquired on 04 August 2013 (Figure 2 and Figure 3). The LST in winter case (16 December 2021) showed less variation among the residential communities. Meanwhile, in two summer cases, the OCU presented relatively higher LST, and the VC was provided with the lowest LST. Generally, similar patterns (inter-class difference and intra-class variation) between Greenness and NDVI were observable, although their actual values differed. In further investigation, NDVI was only used as indicator of vegetation (Figure 3 and Figure 5). The VC had the largest NDVI (Greenness) followed by the MC, while the NCU shared lower vegetation with the OCU. On average, the NCU was likely higher in the Wetness component, and the MC was the lowest one potentially. Although the residential communities showed seasonal variation in biophysical variables more or less, the relative ranking among them was consistent.

In the summer cases, for all individual types except the OCU on 04 August 2013, NDVI and the Wetness component both showed negative relationship with LST (Figure 3 and Figure 4). Nevertheless, the individual relationships between biophysical components or spectral index (i.e. the Wetness component or NDVI) and LSTs varied among the residential community types. In particular, the observable differences in slope of the linear trend (Figure 3 and Figure 4) suggest the cooling effects of NDVI (or the Wetness component) on four types were different in summer.
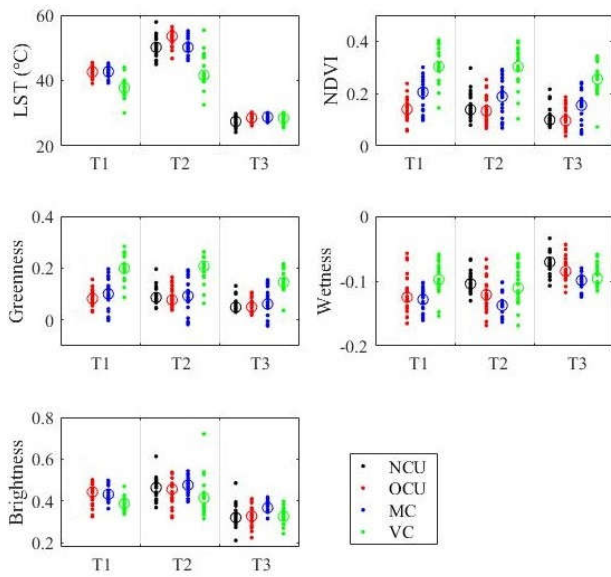
Figure 2. Comparisons among four types of residential community in LST and related variables, including Greenness, Wetness, Brightness, and NDVI. T1, T2, and T3 indicate the date of imagery acquisitions, which were 04 August 2013, 25 July and 16 December 2021 respectively. The NCU communities were not considered on T1. In this figure, the dots represent the values of corresponding variable for individual communities, while the circles indicate the median values correspondingly.
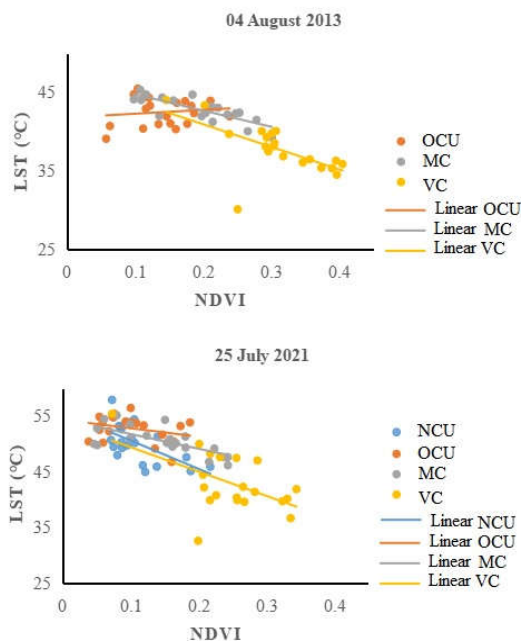

Figure 3. LST *vs* NDVI for different residential community types as recorded by two specific observations of the Landsat-8 OLI/TIRS, acquired on 04 August 2013 and 25 July 2021 respectively. The NCU communities were not considered in analyzing the data acquired on 04 August 2013.

Compared with the NCU, the OCU was generally characterized with lower NDVI and Wetness component, which therefore had higher LST (Figure 2—Figure 4). The MC was equivalent to the NCU in terms of LST although it had higher NDVI, which possibly was resulted from its lower Wetness component. Furthermore, there were several VCs with high LST, although the majority of the VC had lower LST and was higher in NDVI and Wetness component. As mentioned in Figure 2, seasonal variation in LST and biophysical components (or spectral index) occurred. In the winter case (16 December 2021), differences in LST among four types were minor relative to the inter-class differences in the summer cases. Seasonal variation in the relationships of LST with the factors was also observable, especially for the relationship with NDVI (Figure 3 and Figure 5). Specifically, a significant negative relationship between LST and NDVI was there in the summer cases regardless of residential community types, whereas no significant relationship was observed in the winter case. In contrast to NDVI, the Wetness component showed significant negative relationship with LST in all cases. It suggested that the Wetness component was more effective in predicting surface thermal environment (e.g., LST) over residential community compared against NDVI. In fact, the limitation of NDVI as indicator to model surface temperature was discussed in previous investigation (Yuan and Marvin, 2007).

The preliminary findings on thermal environment over residential community were mainly based on the Landsat-8 OLI/TIRS Collection 2 Level-2 products. The TIRS acquires imagery with a spatial resolution of 100 m nominally, which are resampled to 30 m in delivered data products (Chen et al., 2017). The medium resolution may not be optimal for resolving residential community issues, at which mixed pixels likely occur. In this study, the communities covering large area were selected for investigation. Nevertheless, without considering communities covering relatively small area, biased findings were possible. Since different surface types (objects) usually present different diurnal cycle in temperature (Sun et al., 2020; Jiang et al., 2022), an instantaneous observation recorded by the Landsat-8 TIR is not effective to depict the thermal property of residential community. At the same time, quality of the surface temperature product is important, but the accuracy was not assessed in this study due mainly to the difficulty in obtaining adequate ground true values for the archived Landsat products. Previous investigations mentioned major challenges in estimating surface temperature from the Landsat data especially over urban area (Chen et al., 2016, 2017).

Furthermore, surface landscape is actually characterized with 3D properties rather than 2D. Therefore, factors associated with 3D structure of the objects within and around a residential community possibly affect its thermal environment (Chen et al., 2022). However, the 3D information is insufficiently contained in the TCT based components as well as in spectral index (i.e. NDVI) derived from the Landsat-8 OLI surface reflectance. To further understand the relationship of landscape properties with thermal environment within residential community, simulation tests (e.g., with ENVI-MET) in details are required, besides more observations. As mentioned before, Tong'an District covers wide and complex territory along with different local climate types. The background of geography and climate around individual community may affect its environment (e.g., thermal environment) correspondingly. In this study, impacts of this kind of background was not discussed. In terms of local scale background, the framework of local climate zones (LCZ) has been widely implemented, especially in urban climate (Stewart and Oke, 2012; Bechtel et al., 2019). Considering the LCZ in analyzing the thermal environment of residential community will improve further the preliminary study.
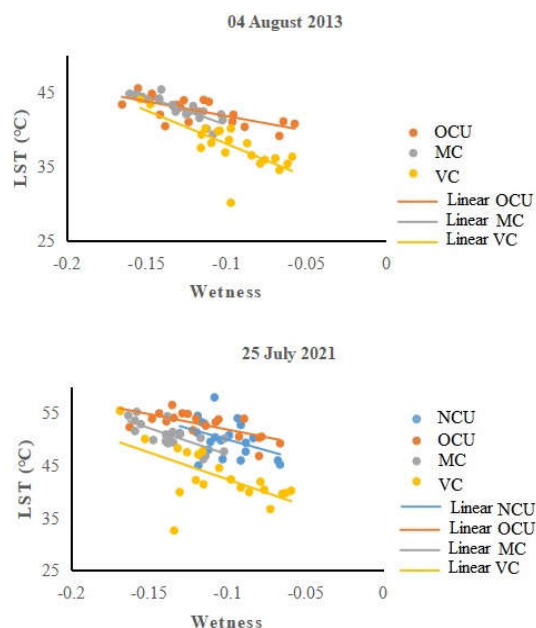
Figure 4. LST *vs* TCT based Wetness for different residential community types as recorded by two specific observations of the Landsat-8 OLI/TIRS, acquired on 04 August 2013 and 25 July 2021 respectively.
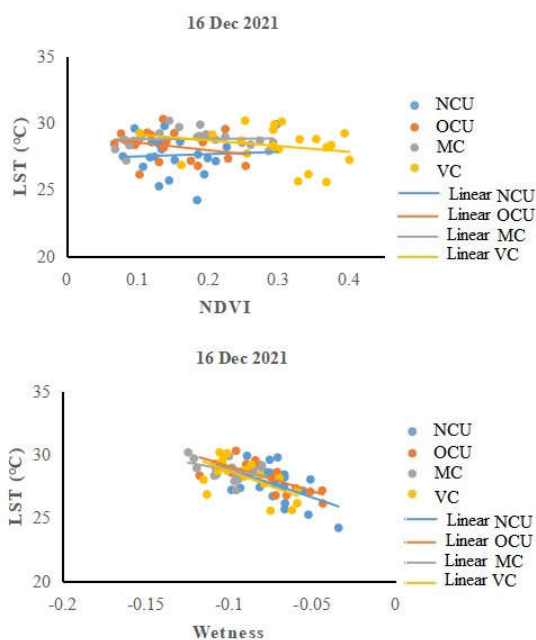

Figure 5. LST *vs* NDVI and TCT based Wetness for different residential community types as recorded by a specific observation of the Landsat-8 OLI/TIRS acquired on 16 December 2021.

4. CONCLUSIONS

In summary, the comparisons in biophysical factors and LST among four residential community types over Tong'an District were discussed, mainly based on three scenes of the Landsat-8

OLI/TIRS Collection 2 Level-2 products. Specifically, the OCU was generally provided with lower NDVI and Wetness component, which therefore had higher LST. Different relationships of LST with biophysical factors were observed among the residential community types. In particular, the findings suggested that cooling effects of NDVI (or the Wetness component) on residential community were different among four types in summer. At the same time, seasonal variation in these relationships was demonstrated, especially in the relationship of LST with NDVI. Compared with NDVI, the Wetness component was more effective in predicting surface thermal environment (e.g., LST) over residential community. Furthermore, the preliminary investigation showed that the residential communities located in rural-urban fringe and several village communities had confronted with problems in thermal environment as well as in surface biophysical conditions. Accordingly, in addition to the UHI widely discussed for urban area, the thermal environment over the areas (i.e. rural-urban fringe and village) away from urban centers should also deserve much attention. More investigations are required to understand fully the thermal environment of residential communities over this coastal region which covers complex territory and different local climate types, to improve the living quality accordingly.

REFERENCES

Bechtel, B., Demuzere, M., Mills, G., Zhan, W.F., Sismanidis, P., Small, C., Voogt, J., 2019. SUHI analysis using Local Climate Zones—A comparison of 50 cities. *Urban Climate* 28, 100451.

Chen, F., Yang, S., Su, Z., Wang, K., 2016. Effect of emissivity uncertainty on surface temperature retrieval over urban areas: Investigations based on spectral libraries. *ISPRS Journal of Photogrammetry and Remote Sensing* 114, 53-65.

Chen, F., Yang, S., Yin, K., Chan, P., 2017. Challenges to quantitative applications of Landsat observations for the urban thermal environment. *Journal of Environmental Sciences* 59, 80-88.

Chen, F., Lou, S., Fan, Q., Wang, C., Claverie, M., Wang, C., Li, J., 2019. Normalized difference vegetation index continuity of the Landsat 4-5 MSS and TM: Investigations based on simulation. *Remote Sensing* 11(14), 1681.

Chen, F., Fan, Q., Lou, S., Yang, L., Wang, C., Claverie, M., Wang, C., Junior, J.M., Gonçalves, W.N., Li, J., 2020. Characterization of MSS channel reflectance and derived spectral indices for building consistent Landsat 1-5 data record. *IEEE Transactions on Geoscience and Remote Sensing* 58(12), 8967-8984.

Chen, C.M., Bagan, H., Yoshida, T., Borjigin, H., Gao, J., 2022. Quantitative analysis of the building-level relationship between

building form and land surface temperature using airborne LiDAR and thermal infrared data. *Urban Climate* 45, 101248.

Cook, M., Schott, J.R., Mandel, J., Raqueno, N., 2014. Development of an operational calibration methodology for the Landsat thermal data archive and initial testing of the atmospheric compensation component of a Land Surface Temperature Product from the archive. *Remote Sensing* 6(11), 11244-11266.

Crist, E.P., Cicone, R.C., 1984. A physically-based transformation of Thematic Mapper data ─ The TM tasseled cap. *IEEE Transactions on Geoscience and Remote Sensing* 22(3), 256-263.

Du, H.L., Zhan, W.F., Liu, Z.H., Li, J.F., Li, L., Lai, J.M., Miao, S.Q., Huang, F., Wang, C.G., Wang, C.L., Fu, H.Y., Jiang, L., Hong, F.L., Jiang, S.D., 2021. Simultaneous investigation of surface and canopy urban heat islands over global cities. *ISPRS Journal of Photogrammetry and Remote Sensing* 181, 67-83.

García-Santos, V., Cuxart, J., Martínez-Villagrasa, D., Jiménez, M.A., Simó, G., 2018. Comparison of three methods for estimating land surface temperature from Landsat 8-TIRS sensor data. *Remote Sensing* 10(9), 1450.

Jiménez-Muñoz, J.C., Sobrino, J.A., Skoković, D., Mattar, C., Cristóbal, J., 2014. Land surface temperature retrieval methods from Landsat-8 thermal infrared sensor data. *IEEE Geoscience and Remote Sensing Letters* 11(10), 1840-1843.

Jiang, L., Zhan, W.F., Tu, L.L., Dong, P., Wang, S.S., Li, L., Wang, C.L., Wang, C.G., 2022. Diurnal variations in directional brightness temperature over urban areas through a multi-angle UAV experiment. *Building and Environment* 222, 109408.

Patz, J.A., Campbell-Lendrum, D., Holloway, T., Foley, J.A., 2005. Impact of regional climate change on human health. *Nature* 438(17), 310-317.

Stewart, I.D., Oke, T.R., 2012. Local Climate Zones for urban temperature studies. *Bulletin of the American Meteorological Society* 93(12), 1879-1900.

Sun, J., Mao, Z.H., Wang, L., Deng, L., 2020. Diurnal variation and mutual influence of typical ground objects' thermal environment in residential areas. *Journal of Geo-information Science* 22(2), 279-289.

United States Geological Survey (USGS), 2022. Landsat 8-9 Collection 2 (C2) Level 2 Science Product (L2SP) Guide. LSDS-1696 (Version 4.0), EROS, Sioux Falls, South Dakota.

Voogt, J., Oke, T.R., 2003. Thermal remote sensing of urban climates. *Remote Sensing of Environment* 86(3), 370-384.

Weng, Q., 2009. Thermal infrared remote sensing for urban climate and environmental studies: methods, applications, and trends. *ISPRS Journal of Photogrammetry and Remote Sensing* 64(4), 335-344.

Wilson, J.S., Clay, M., Martin, E., Stuckey, D., Vedder-Risch, K., 2003. Evaluating environmental influences of zoning in urban ecosystems with remote sensing. *Remote Sensing of Environment* 86(3), 303-321.

Yuan, F., Marvin, E., 2007. Comparison of impervious surface area and normalized difference vegetation index as indicators of surface urban heat island effects in Landsat imagery. *Remote Sensing of Environment* 206(3), 375-386.

Zhai, Y.G., Roy, D.P., Martins, V.S., Zhang, H.K., Yan, L., Li, Z.B., 2022. Conterminous United States Landsat-8 top of atmosphere and surface reflectance tasseled cap transformation coefficients. *Remote Sensing of Environment* 274, 112992.